

---

This is an electronic reprint of the original article.  
This reprint may differ from the original in pagination and typographic detail.

Motohashi, T.; Nonaka, Y.; Sakai, K.; Karppinen, M.; Yamauchi, H.

## Fabrication and thermoelectric characteristics of [(Bi,Pb)<sub>2</sub>Ba<sub>2</sub>O<sub>4±w</sub>]<sub>0.5</sub>CoO<sub>2</sub> bulks with highly aligned grain structure

*Published in:*  
Journal of Applied Physics

*DOI:*  
[10.1063/1.2838161](https://doi.org/10.1063/1.2838161)

Published: 01/01/2008

*Document Version*  
Publisher's PDF, also known as Version of record

*Please cite the original version:*

Motohashi, T., Nonaka, Y., Sakai, K., Karppinen, M., & Yamauchi, H. (2008). Fabrication and thermoelectric characteristics of [(Bi,Pb)<sub>2</sub>Ba<sub>2</sub>O<sub>4±w</sub>]<sub>0.5</sub>CoO<sub>2</sub> bulks with highly aligned grain structure. *Journal of Applied Physics*, 103(3), 1-6. Article 033705. <https://doi.org/10.1063/1.2838161>

---

This material is protected by copyright and other intellectual property rights, and duplication or sale of all or part of any of the repository collections is not permitted, except that material may be duplicated by you for your research use or educational purposes in electronic or print form. You must obtain permission for any other use. Electronic or print copies may not be offered, whether for sale or otherwise to anyone who is not an authorised user.

# Fabrication and thermoelectric characteristics of $[(\text{Bi, Pb})_2\text{Ba}_2\text{O}_{4\pm w}]_{0.5}\text{CoO}_2$ bulks with highly aligned grain structure

T. Motohashi, Y. Nonaka, and K. Sakai, M. Karppinen and H. Yamauchi

Citation: *Journal of Applied Physics* **103**, 033705 (2008); doi: 10.1063/1.2838161

View online: <http://dx.doi.org/10.1063/1.2838161>

View Table of Contents: <http://aip.scitation.org/toc/jap/103/3>

Published by the American Institute of Physics

---

---

**AIP** | Journal of  
Applied Physics

Save your money for your research.  
It's now **FREE** to publish with us -  
no page, color or publication charges apply.

Publish your research in the  
*Journal of Applied Physics*  
to claim your place in applied  
physics history.

# Fabrication and thermoelectric characteristics of $[(\text{Bi}, \text{Pb})_2\text{Ba}_2\text{O}_{4\pm w}]_{0.5}\text{CoO}_2$ bulks with highly aligned grain structure

T. Motohashi,<sup>a)</sup> Y. Nonaka, and K. Sakai

*Materials and Structures Laboratory, Tokyo Institute of Technology, Yokohama 226-8503, Japan*

M. Karppinen and H. Yamauchi

*Materials and Structures Laboratory, Tokyo Institute of Technology, Yokohama 226-8503, Japan and Laboratory of Inorganic and Analytical Chemistry, Helsinki University of Technology, P.O. Box 6100, FI-02015 TKK, Finland*

(Received 3 June 2007; accepted 29 November 2007; published online 7 February 2008)

Here, we report fabrication and thermoelectric characteristics of polycrystalline bulks with aligned grains of the misfit-layered cobalt oxides,  $[(\text{Bi}_{1-x}\text{Pb}_x)_2\text{Ba}_2\text{O}_{4\pm w}]_{0.5}\text{CoO}_2$ . High-quality precursor powder was prepared with a spray-drying technique. The precursor was then sintered under a uniaxial pressure to yield dense bulk samples consisting of highly aligned grains. The electrical conductivity of such samples was four times higher than that of conventionally sintered bulks. Accordingly, the thermoelectric characteristics of the grain-aligned specimens were enhanced.

© 2008 American Institute of Physics. [DOI: 10.1063/1.2838161]

## I. INTRODUCTION

Upon confronting the global warming problem, human beings have begun to recognize the importance of power generation using “thermoelectrics.”<sup>1</sup> Thermoelectrics are materials which can directly convert a heat flow to an electric current and vice versa. Such materials enable us to generate electric power using waste heat from, e.g., automobiles and, therefore, contribute to enhancing efficiency of energy utilization. The efficiency of a thermoelectric (TE) material is assessed with a figure of merit  $Z$  defined as  $S^2/\rho\kappa$ , where  $S$  is the Seebeck coefficient,  $\rho$  the electrical resistivity, and  $\kappa$  the thermal conductivity. For practical applications, the nondimensional parameter as defined by  $ZT$  is desired to be higher than unity.<sup>1</sup>

In recent years, “misfit-layered cobalt oxides” have been highlighted as next-generational TE materials.<sup>2–6</sup> The members of this material family possess a crystal structure consisting of alternate stacks of a hexagonal  $\text{CoO}_2$  layer (of the  $\text{CdI}_2$  structure) and a multi-square-plane layer,  $M_m\text{A}_2\text{O}_{2+m\pm w}$  [of the rock-salt (RS) structure]. The general chemical formula may be given by  $[(M_m\text{A}_2\text{O}_{2+m\pm w})_q\text{CoO}_2]$  ( $M=\text{Bi}, \text{Pb}, \text{Co}, \text{etc.}$ ,  $A=\text{Ba}, \text{Sr}, \text{etc.}$ ,  $m=0, 1, \text{ or } 2$ ), where  $q$  is the ratio of  $b$ -axis lengths of the two layers, i.e.,  $q = b_{\text{CoO}_2}/b_{\text{RS}}$ . Noticeable is that the two layers are incoherently or “misfittingly” coupled with each other along the  $b$  axis such that the  $q$  value is often fractional.<sup>7,8</sup> This “nanocomposite” structure consisting of highly conductive  $\text{CoO}_2$  layers and insulating RS layers is essential for the superb TE characteristics of misfit-layered cobalt oxides. In fact, single crystalline samples of some misfit-layered materials have been reported to possess high values of figure of merit, e.g.,  $ZT \approx 1.0$ , at temperatures above  $500^\circ\text{C}$ .<sup>9,10</sup> Nevertheless, it has been known that the  $ZT$  value is significantly lower for polycrys-

talline samples. This is because electrical resistivity is much higher for polycrystalline bulks than for certain orientation(s) of single crystals.

To improve the thermoelectric properties of polycrystalline bulks, grain texturing has been considered to be effective: Matsubara *et al.*<sup>11</sup> fabricated a grain-aligned bulk sample of  $[(\text{Ca}, \text{Bi})_2\text{CoO}_{3-w}]_{0.62}\text{CoO}_2$  through uniaxial pressure sintering to yield  $ZT=0.29$  at  $700^\circ\text{C}$ , being much higher than those for conventionally sintered samples. Xu *et al.*<sup>12</sup> also reported an excellent TE performance ( $ZT=0.32$  at  $730^\circ\text{C}$ ) for a Bi/Na-substituted  $[\text{Ca}_2\text{CoO}_{3-w}]_{0.62}\text{CoO}_2$  bulk with aligned grains. So far, optimization regarding the microstructure of polycrystalline bulks has been achieved only for  $[\text{Ca}_2\text{CoO}_{3-w}]_{0.62}\text{CoO}_2$  as well as for some of its analogs.

Recently, we reported<sup>13,14</sup> that the misfit-layered cobalt oxides,  $[(\text{Bi}_{1-x}\text{Pb}_x)_2\text{Ba}_2\text{O}_{4\pm w}]_{0.5}\text{CoO}_2$ , are promising candidates for high-efficiency TE materials. The  $[(\text{Bi}_{1-x}\text{Pb}_x)_2\text{Ba}_2\text{O}_{4\pm w}]_{0.5}\text{CoO}_2$  phases possess double (Bi, Pb)O planes in the RS block (Fig. 1): this is the case of  $M=(\text{Bi}, \text{Pb})$ ,  $A=\text{Ba}$ , and  $m=2$  in the general chemical formula.

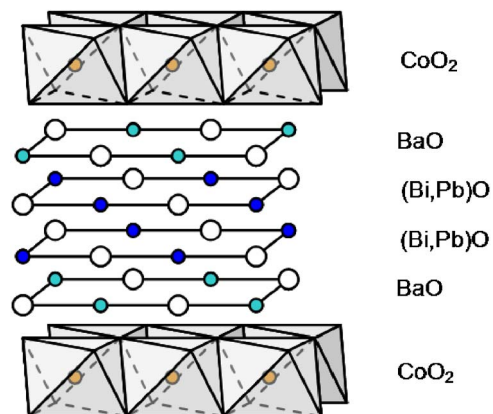


FIG. 1. (Color online) Schematic crystal structure of  $[(\text{Bi}_{1-x}\text{Pb}_x)_2\text{Ba}_2\text{O}_{4\pm w}]_{0.5}\text{CoO}_2$ .

<sup>a)</sup>Electronic mail: t-mot@mssl.titech.ac.jp.

They exhibit reasonably high metallic conductivity, high Seebeck coefficients ( $S \approx 120 \mu\text{V}/\text{K}$  at room temperature) and low thermal conductivity ( $\kappa \approx 1 \text{ W}/\text{m K}$  between room temperature and  $630 \text{ }^\circ\text{C}$ ).<sup>13,14</sup> It should be noted that the temperature where the resistivity upturn occurs is significantly low, i.e.,  $\sim 53$  and  $26 \text{ K}$  for  $x=0.1$  and  $0.2$  samples, respectively, in comparison with those of other misfit-layered cobalt oxides, e.g.,  $80 \text{ K}$  of  $[\text{Ca}_2\text{CoO}_{3-\omega}]_{0.62}\text{CoO}_2$ .<sup>4,5</sup> Although the value  $ZT \approx 0.03$  (at  $530 \text{ }^\circ\text{C}$  for  $x=0.2$ )<sup>14</sup> is far below the value sufficient for practical uses ( $ZT \approx 1$ ), it signals that the material is definitely attractive provided that it could be made into a textured bulk form. In the present work, we fabricated  $[(\text{Bi}_{1-x}\text{Pb}_x)_2\text{Ba}_2\text{O}_{4\pm w}]_{0.5}\text{CoO}_2$  polycrystalline bulks consisting of highly textured grains and characterized the TE properties. Electrical conductivity of the textured bulk increased up to four times as compared to that of a nontextured bulk. This accordingly enhanced the thermoelectric characteristics.

## II. EXPERIMENTAL

Reagent grade  $\text{Bi}_2\text{O}_3$ ,  $\text{Pb}(\text{NO}_3)_2$ ,  $\text{Ba}(\text{NO}_3)_2$ , and  $\text{Co}(\text{NO}_3)_2 \cdot 6\text{H}_2\text{O}$  powders were weighed to achieve the molar ratios of  $\text{Bi}:\text{Pb}:\text{Ba}:\text{Co}=(1-x):x:0.9:1.1$  ( $x=0, 0.1, 0.2$ ) and then dissolved in  $\text{HNO}_3$ . To obtain a powder mixture more homogeneous than mechanically mixed powders, the solution was spray dried using a commercial machine (BÜCHI, B-290). The spray-dried powder was preheated at  $475 \text{ }^\circ\text{C}$  in flowing air to get rid of  $\text{NO}_x$  gas and moisture. The powder was then calcined at  $710 \text{ }^\circ\text{C}$  for 12 h in  $0.1\%-\text{O}_2/\text{Ar}$  gas flow. Low-oxygen-partial-pressure heat treatment is a must for obtaining a  $[(\text{Bi}_{1-x}\text{Pb}_x)_2\text{Ba}_2\text{O}_{4\pm w}]_{0.5}\text{CoO}_2$  bulk of x-ray diffraction (XRD)-purity.<sup>13</sup>

Grain texturing for the  $[(\text{Bi}_{1-x}\text{Pb}_x)_2\text{Ba}_2\text{O}_{4\pm w}]_{0.5}\text{CoO}_2$  bulks was processed utilizing a homemade machine for hot pressing a pellet under a controlled oxygen pressure. The calcined powder was first cold pressed into a pellet of  $20 \text{ mm}$  in diameter, and then the pellet was placed in the hot-press machine for sintering in flowing  $0.1\%-\text{O}_2/\text{Ar}$  gas applying a uniaxial pressure of  $\sim 40 \text{ MPa}$ . To find out the optimal conditions for grain texturing, several pellet samples were hot pressed for 12 h at various temperatures ( $650\text{--}775 \text{ }^\circ\text{C}$ ).

The cation compositions of the precursor powder and of the hot-pressed (“HP”) bulk samples were determined by inductively coupled plasma atomic emission spectroscopy (ICP-AES). By XRD (Rigaku RINT-2000V equipped with a rotating anode,  $\text{Cu } K_\alpha$  radiation), phase purity of the HP samples was monitored and the degree of grain alignment was determined. Microstructural observations were made with a scanning electron microscope (SEM) (Hitachi S-4500 equipped with an energy dispersive analyzer). Electrical resistivity and Seebeck coefficient were measured in a temperature range of  $5\text{--}300 \text{ K}$  employing a four-probe technique (Quantum Design, physical property measurement system) and a steady-state technique, respectively.

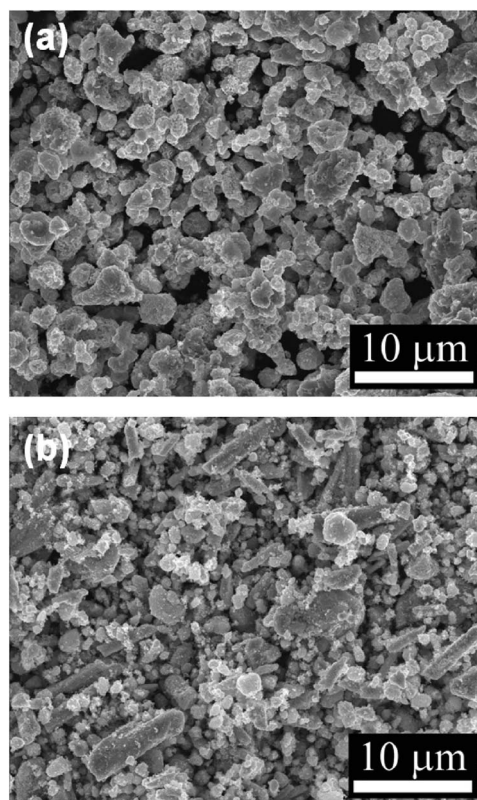


FIG. 2. SEM images of precursor powders for  $[(\text{Bi}_{1-x}\text{Pb}_x)_2\text{Ba}_2\text{O}_{4\pm w}]_{0.5}\text{CoO}_2$  ( $x=0.2$ ): (a) spray-dried and heated (at  $475 \text{ }^\circ\text{C}$  in air) powder and (b) mechanically mixed powder.

## III. RESULTS AND DISCUSSION

### A. Precursor powders

For precise control of particle size of the spray-dried powder, conditions used for the spray drying were carefully optimized. It was found that the higher feeding speed, the higher concentration of nitrate solution, and the lower spray-gas flow rate yielded the smaller sized particles. It was essential that every adjustable parameter is recalibrated whenever some other parameters are changed in order to avoid the lower product yields. With a set of optimized parameters, we were able to obtain fine and homogeneous precursor powders with a relatively high yield of  $\sim 60 \text{ wt } \%$ .

In Fig. 2(a), a typical SEM image of the spray-dried powder (of the  $x=0.2$  sample preheated at  $475 \text{ }^\circ\text{C}$ ) is shown. It is seen that the powder consists of agglomerates of fine particles ( $\sim 300 \text{ nm}$  in diameter). The flat contrast of the image indicates that the constituent elements are homogeneously distributed. This is in contrast to the case of a mechanically mixed powder, as shown in Fig. 2(b), in which bright and dark grains of different sizes are mixed, suggesting that the starting powder was inhomogeneous in terms of chemical composition. To evaluate the degree of compositional homogeneity, SEM–energy dispersive spectroscopy (EDS) analysis was performed for both the spray-dried and the mechanically mixed powders. For each powder,  $(\text{Bi}, \text{Pb})/\text{Ba}/\text{Co}$  ratios were measured at 45 spots in an area of  $5 \times 5 \mu\text{m}^2$ . The standard deviations of the atomic ratios were  $\sigma = 3.8\% \text{--} 6.0\%$  and  $10.0\% \text{--} 18.9\%$  for the former and

TABLE I. Cation ratios determined by ICP-AES for hot-pressed samples of  $[(\text{Bi}_{1-x}\text{Pb}_x)_2\text{Ba}_2\text{O}_{4\pm w}]_{0.5}\text{CoO}_2$ .

Sample	Nominal composition Bi:Pb:Ba:Co	Analyzed composition Bi:Pb:Ba:Co
$x=0$	1.00:0.00:0.90:1.10	1.00:0.00:0.93:1.12
$x=0.1$	0.90:0.10:0.90:1.10	0.91:0.09:0.91:1.13
$x=0.2$	0.80:0.20:0.90:1.10	0.80:0.20:0.97:1.23

the latter powders, respectively, indicating that the spray dried powder is indeed chemically more homogeneous.<sup>15</sup>

Thanks to the excellent compositional homogeneity of the spray-dried powder, the calcined powder (at 710 °C) was essentially single phase of  $[(\text{Bi}_{1-x}\text{Pb}_x)_2\text{Ba}_2\text{O}_{4\pm w}]_{0.5}\text{CoO}_2$ . Note that the calcination temperature is  $\sim 90$  °C lower than that in a conventional solid state reaction method: mechanically mixed powders need to be calcined at a high temperature of 800 °C to obtain single-phase products.<sup>13</sup> A spray-drying technique was previously used for synthesizing (Bi,Pb)-2223 superconductors by Van Driessche *et al.*,<sup>16</sup> who concluded that the technique is useful in fabricating (Bi,Pb)-2223 precursors of improved homogeneity, stoichiometry, particle size, and particle distribution; the spray-dried precursor powders enabled them to obtain (Bi,Pb)-2223 samples of >96% purity even with short calcining/sintering periods. Their conclusions are parallel with ours of the present case of  $[(\text{Bi}_{1-x}\text{Pb}_x)_2\text{Ba}_2\text{O}_{4\pm w}]_{0.5}\text{CoO}_2$ .

The results of chemical composition analyses by means of ICP-AES are summarized in Table I. The cation ratios are in good agreement with the nominal ones for all the single-phase samples, indicating that no selective cation losses occurred during the synthesis procedure. The “Co-rich and Ba-poor atomic ratios,” i.e., Bi:Pb:Ba:Co  $\approx 1-x:x:0.9:1.1$ , may suggest that the Ba site in the RS block is partially substituted by Co, but no evidence for such cation nonstoichiometry in this system has been obtained. We, therefore, adopt the original chemical formula,  $[(\text{Bi}_{1-x}\text{Pb}_x)_2\text{Ba}_2\text{O}_{4\pm w}]_{0.5}\text{CoO}_2$ , for the present samples.

## B. Grain texturing

Since the  $[(\text{Bi}_{1-x}\text{Pb}_x)_2\text{Ba}_2\text{O}_{4\pm w}]_{0.5}\text{CoO}_2$  phase crystallizes in a highly anisotropic form, the microstructure of polycrystalline bulks may be controlled by employing a uniaxial-pressure sintering technique, as in the case of superconductive (Bi,Pb)-2223 bulks.<sup>17,18</sup> SEM observations of the present samples have shown that the uniaxial-pressure sintering effectively works for our cobalt oxides,  $[(\text{Bi}_{1-x}\text{Pb}_x)_2\text{Ba}_2\text{O}_{4\pm w}]_{0.5}\text{CoO}_2$  (Fig. 3). In both  $x=0$  and 0.2 HP samples, platelike grains are aligned along the flat surface perpendicular to the pressure direction, being in sharp contrast to that observed for conventionally sintered (“CS”) samples in which crystallites were randomly oriented with voids between the grains. The density of the  $x=0.2$  HP sample was determined by means of Archimedes’ method to be  $7.06 \pm 0.07$  g/cm<sup>3</sup>. This value corresponds to a packing density of 0.99(1) under an assumption that the sample is oxygen stoichiometric: the theoretical density is 7.14 g/cm<sup>3</sup>. We were not able to determine the density of the CS sample

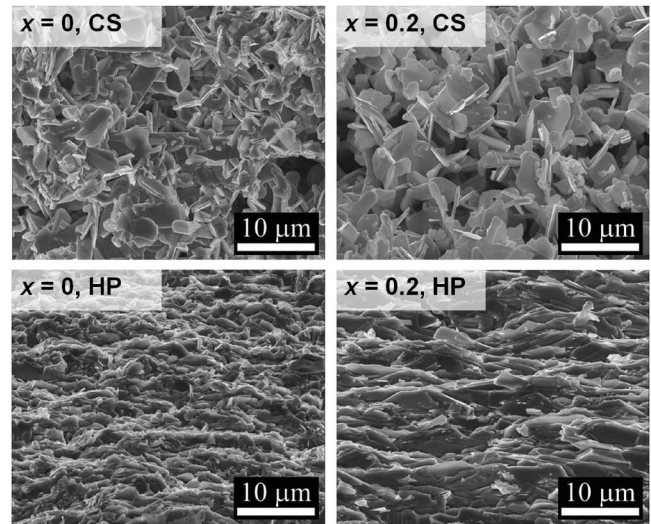


FIG. 3. SEM images of  $[(\text{Bi}_{1-x}\text{Pb}_x)_2\text{Ba}_2\text{O}_{4\pm w}]_{0.5}\text{CoO}_2$  bulk samples: in left column,  $x=0$  conventionally sintered (“CS”) and hot-pressed (“HP”) samples, and in right column,  $x=0.2$  CS and HP samples. To obtain HP samples, a uniaxial pressure was applied perpendicular to the grain-elongation direction.

with Archimedes’ method due to its highly porous microstructure. The enhanced density of the HP sample is most likely due to the highly aligned grain structure.

Figure 4 shows the XRD patterns for the  $x=0.2$  CS and HP (polished) surfaces. The CS sample shows a typical random grain structure. On the contrary, the HP sample shows diffraction peaks only with  $hk_1lk_2=00l0$  (where  $k_1$  and  $k_2$  are the  $k$  Miller indices corresponding to the RS and the  $\text{CoO}_2$  block, respectively). This indicates a high grain orientation along the crystallographic  $c$  axis. The degree of grain alignment was determined employing Lotgering’s method.<sup>19</sup> The orientation factor  $F$  (i.e., “Lotgering’s factor”) is defined as

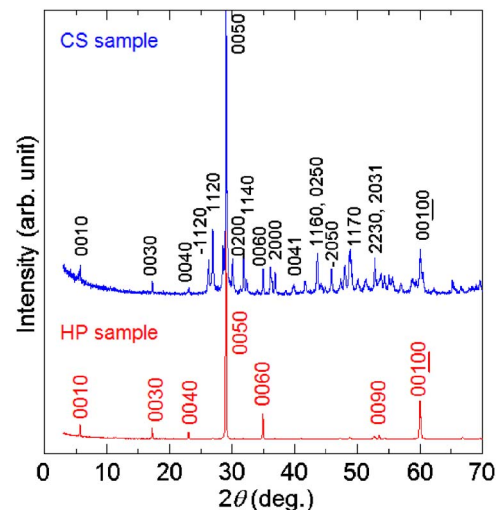


FIG. 4. (Color online) X-ray diffraction patterns for the  $x=0.2$  CS (top) and HP (bottom) samples. The pattern for the HP sample was taken at the polished surface perpendicular to the pressure direction. Note that the four-integer indices given in this figure are in the form of  $hk_1lk_2$  ( $k_1$  and  $k_2$  are Miller indices corresponding to the RS and  $\text{CoO}_2$  blocks, respectively).

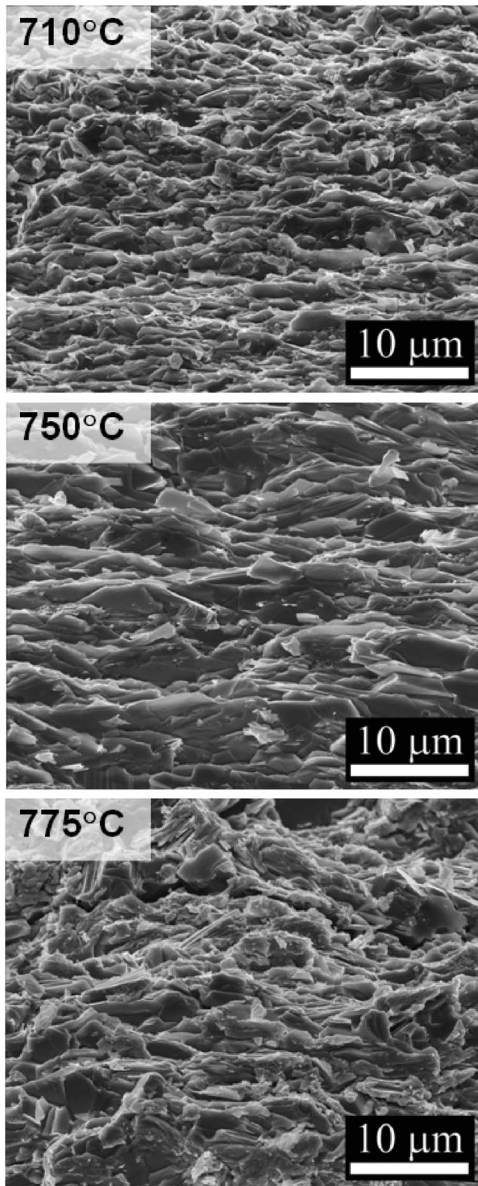


FIG. 5. SEM images of the  $x=0.2$  HP samples fired at 710, 750, and 775 °C.

$$F \equiv (P - P_0)/(1 - P_0),$$

where  $P = \Sigma I(00l0)/\Sigma I(hk_1lk_2)$  and  $P_0 = \Sigma I_0(00l0)/\Sigma I_0(hk_1lk_2)$  are calculated for the  $c$ -axis oriented and the nonoriented bulk samples, respectively. We performed calculations using peaks in a  $2\theta$  range of 3°–60° and obtained  $F = 0.98$  for the HP sample. This is close to the highest  $F$  value previously reported for some similar cobalt oxide bulks.<sup>20</sup>

Next, we studied the effect of hot-pressing temperature on the bulk microstructure. Shown in Fig. 5 are SEM images of the  $x=0.2$  HP samples sintered at 710, 750, and 775 °C for 12 h. For the samples sintered at 710 and 750 °C, plate-like grains are uniformly oriented along the perpendicular direction to the pressure application. Comparison between the latter two samples (the upper and middle figures in Fig. 5) evidences a significant enhancement in the grain growth with increasing temperature. However, the temperature was too high for optimum grain texturing, as the grain alignment

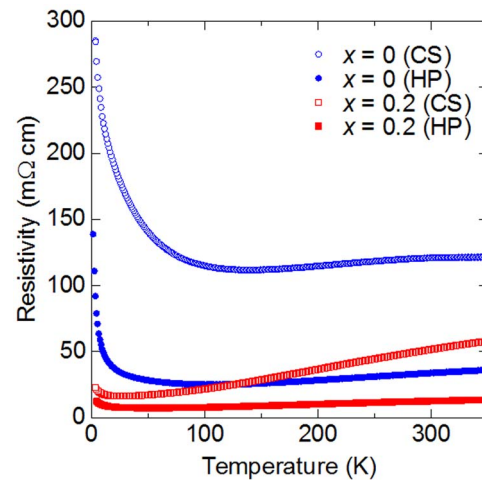


FIG. 6. (Color online) Dependences of electrical resistivity on temperature for the CS (open symbols) and HP (solid symbols) samples with  $x=0$  (blue circles) and 0.2 (red squares).

is partly disrupted in the sample sintered at 775 °C, as seen in Fig. 5. This may have been caused by some phase decomposition at high temperatures. Lotgering's factor is indeed smaller for this sample ( $F=0.95$ ) than for the others ( $F=0.98$ ), which is consistent with the SEM observations.

The high value of the  $F$  factor for the present HP samples is considered to have been achieved for the reasons as follows. (1) The highly anisotropic form of the original crystallites is favorable for grain texturing under a uniaxial pressure, as proven for superconductive Bi-based layered copper oxides. (2) Sample sintering at a temperature just below the decomposition point significantly accelerates the grain growth and grain-boundary sliding.<sup>21</sup>

### C. Thermoelectric characteristics

Among the three parameters, i.e., Seebeck coefficient ( $S$ ), electrical resistivity ( $\rho$ ), and thermal conductivity ( $\kappa$ ), which are involved with the TE figure of merit,  $\rho$  is the most sensitively affected by the microstructure of bulk samples. Figure 6 displays electrical resistivity data for the CS and HP samples fired at the same temperature of 750 °C. For the HP sample, resistivity was measured with an applied current perpendicular to the pressure direction. The magnitude of  $\rho$  in this direction is drastically reduced for the HP sample. The values of  $\rho$  at 300 K are 33.5 and 12.2 mΩ cm for the  $x=0$  and 0.2 HP samples, respectively. These values are smaller by a factor of 1/4 compared to those for the corresponding CS samples, i.e., 120.7 and 51.3 mΩ cm, respectively.

In Fig. 7, the resistivity at 300 K ( $\rho_{300\text{ K}}$ ) is plotted as a function of the hot-pressing/firing temperature for the  $x=0$  and 0.2 HP samples. For the case of  $x=0$  (i.e., Pb-free), the  $\rho_{300\text{ K}}$  value monotonously decreases with increasing temperature up to 775 °C. The reduced resistivity is apparently due to the decrease in the density of weak links along the electrical current path, which is achieved by uniaxial sintering at elevated temperatures. On the other hand,  $\rho_{300\text{ K}}$  for the case of  $x=0.2$  rapidly decreases as the firing temperature increases from 650 to 750 °C and starts to rather increase at above 750 °C. In correspondence with this, the  $F$  value

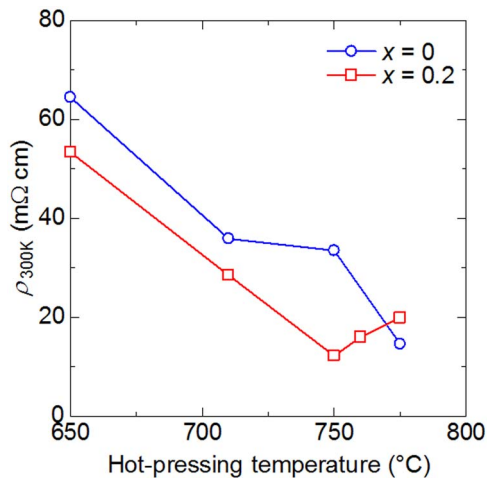


FIG. 7. (Color online) Resistivity at 300 K ( $\rho_{300\text{K}}$ ) of the  $x=0$  (blue circles) and 0.2 (red squares) samples as a function of hot-pressing/firing temperature.

reaches a maximum at about 750 °C and starts to decrease at higher temperatures. This is probably due to phase decomposition at above 750 °C. Thus, hot pressing of the sample at temperatures just beneath the decomposition point is the most effective to achieve the optimal electrical transport property.

Figure 8 shows the dependence of Seebeck coefficient  $S$  on temperature for the CS (open symbols) and HP (solid symbols) samples fired at 750 °C. For both samples with  $x=0$  (Pb free) and  $x=0.2$  (Pb-substituted), the Seebeck coefficient values are nearly equal throughout the temperature region of the measurement. This would imply that the microstructure of the sample does not significantly affect the  $S$  value, reflecting the fact that thermoelectric power is a bulk property and little sensitive to interface/surface characteristics. Thanks to the reduced value of  $\rho$  and the invariant  $S$  value, the TE power factor as defined by  $P \equiv S^2/\rho$  was significantly enhanced (by four times). In fact, the  $P$  values at 300 K were 0.28 (0.083) and 1.2 (0.39)  $\mu\text{W cm}^{-1} \text{K}^{-2}$ , respectively, for  $x=0.2$  ( $x=0$ ) CS and HP samples.<sup>22</sup>

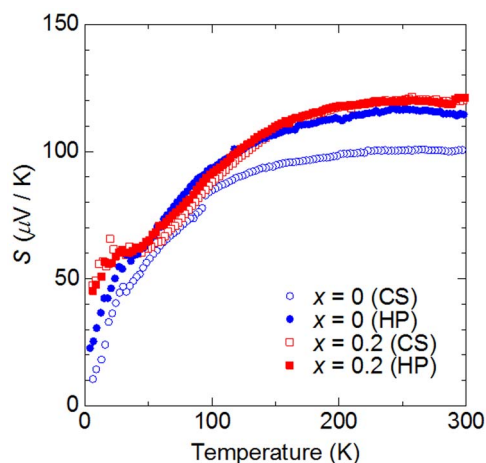


FIG. 8. (Color online) Dependences of the Seebeck coefficient ( $S$ ) on temperature for the CS (open symbols) and HP (solid symbols) samples with  $x=0$  (blue circles) and 0.2 (red squares).

## IV. CONCLUSION

Bulk samples of the misfit-layered cobalt oxides,  $[(\text{Bi}_{1-x}\text{Pb}_x)_2\text{Ba}_2\text{O}_{4\pm w}]_{0.5}\text{CoO}_2$  with  $x=0, 0.1$ , and 0.2, were synthesized in single phase, and their thermoelectric characteristics were systematically studied. First, high-quality precursor powders were prepared by a spray-drying technique. The spray-dried powders were revealed to be finer and chemically more homogeneous than mechanically mixed powders. To the best of our knowledge, this is the first synthesis of thermoelectric cobalt oxides via spray-dried precursor powders. Then, through subsequent sintering under a uniaxial pressure of  $\sim 40$  MPa, highly dense bulks with strongly aligned grains were successfully fabricated. The highest degree of grain alignment was attained for  $x=0.2$  sample fired at 750 °C, just beneath the phase decomposition temperature. Electrical conductivity of the resultant bulks was boosted up four times as compared with that of conventionally sintered bulk samples. At the same time, the Seebeck coefficient remained rather unchanged, leading to enhancement in thermoelectric characteristics.

## ACKNOWLEDGMENTS

The present work was supported through a research grant from Nissan Motor Co., Ltd. and also through Grant-in-Aid for Scientific Research (No. 16740194) from the Japan Society for the Promotion of Science and by Academy of Finland (Decision No. 110433).

- <sup>1</sup>See, e.g., G. Mahan, B. Sales, and J. Sharp, *Phys. Today* **50**(3), 42 (1997); R. S. Service, *Science* **306**, 806 (2004).
- <sup>2</sup>T. Ito, T. Kawata, T. Kitajima, and I. Terasaki, *Proceedings of the 17th International Conference on Thermoelectrics (ICT' 98)*, Nagoya, Japan, 1998 (unpublished), p. 595.
- <sup>3</sup>S. Li, R. Funahashi, I. Matsubara, K. Ueno, and H. Yamada, *J. Mater. Chem.* **9**, 1659 (1999).
- <sup>4</sup>Y. Miyazaki, K. Kudo, M. Akoshima, Y. Ono, Y. Koike, and T. Kajitani, *Jpn. J. Appl. Phys., Part 2* **39**, L531 (2000).
- <sup>5</sup>A.-C. Masset, C. Michel, A. Maignan, M. Hervieu, O. Toulemonde, F. Studer, and B. Raveau, *Phys. Rev. B* **62**, 166 (2000).
- <sup>6</sup>S. Hébert, S. Lambert, D. Pelloquin, and A. Maignan, *Phys. Rev. B* **64**, 172101 (2001).
- <sup>7</sup>P. Boullay, B. Domengès, M. Hervieu, D. Groult, and B. Raveau, *Chem. Mater.* **8**, 1482 (1996); P. Boullay, R. Seshadri, F. Studer, M. Hervieu, D. Groult, and B. Raveau, *ibid.* **10**, 92 (1998).
- <sup>8</sup>H. Leligny, D. Grebille, O. Pérez, A.-C. Masset, M. Hervieu, C. Michel, and B. Raveau, *C.R. Acad. Sci., Ser. IIC: Chim* **2**, 409 (1999).
- <sup>9</sup>R. Funahashi, I. Matsubara, H. Ikuta, T. Takeuchi, U. Mizutani, and S. Sodeoka, *Jpn. J. Appl. Phys., Part 2* **39**, L1127 (2000).
- <sup>10</sup>R. Funahashi, H. Ikuta, T. Takeuchi, U. Mizutani, I. Matsubara, and M. Shikano, *Oxide Thermoelectrics* (Research Signpost, India, 2002), pp. 83–99.
- <sup>11</sup>I. Matsubara, R. Funahashi, T. Takeuchi, T. Shimizu, S. Sodeoka, Y. Zhou, and K. Ueno, *Oxide Thermoelectrics* (Research Signpost, India, 2002), pp. 101–120.
- <sup>12</sup>G. Xu, R. Funahashi, M. Shikano, I. Matsubara, and Y. Zhou, *Appl. Phys. Lett.* **80**, 3760 (2002).
- <sup>13</sup>K. Sakai, T. Motohashi, M. Karppinen, and H. Yamauchi, *Thin Solid Films* **486**, 58 (2005).
- <sup>14</sup>K. Sakai, M. Karppinen, J. M. Chen, R. S. Liu, S. Sugihara, and H. Yamauchi, *Appl. Phys. Lett.* **88**, 232102 (2006).
- <sup>15</sup>It has been known that results of SEM-EDS analysis are sensitive to the roughness of the analyzed area, sometimes giving incorrect values for the chemical composition of powder samples. In our experiment, however, the effects from the grain roughness are averaged, as the analyzed area (5

$\times 5 \mu\text{m}^2$ ) was much larger than the grain size. Therefore, it is most likely that the standard deviation of the compositional data directly reflects the (compositional) homogeneity of the samples.

- <sup>16</sup>I. Van Driessche, R. Mouton, and S. Hoste, *Mater. Res. Bull.* **31**, 979 (1996).
- <sup>17</sup>N. Murayama, E. Sudo, M. Awano, K. Kani, and Y. Torii, *Jpn. J. Appl. Phys., Part 2* **27**, L1856 (1988); N. Murayama and J. B. Vander Sande, *Physica C* **241**, 235 (1995).
- <sup>18</sup>B. M. Moon, G. Kordas, D. J. van Harlingen, Y. L. Jeng, D. L. Johnson, P. R. Sharpe, and K. Goretta, *Mater. Lett.* **10**, 481 (1991).
- <sup>19</sup>F. K. Lotgering, *J. Inorg. Nucl. Chem.* **9**, 113 (1959).
- <sup>20</sup>M. Sano, S. Horii, I. Matsubara, R. Funahashi, M. Shikano, J. Shimoyama, and K. Kishio, *Jpn. J. Appl. Phys., Part 2* **42**, L198 (2003).
- <sup>21</sup>T. Kimura, T. Yoshimoto, N. Iida, Y. Fujita, and T. Yamaguchi, *J. Am. Ceram. Soc.* **72**, 85 (1989).
- <sup>22</sup>The  $ZT$  values for the  $x=0.2$  and 0 HP samples may be estimated, employing the data for the CS samples of Ref. 14, to be, respectively, 0.033 and 0.013 at 300 K, and 0.13 and 0.037 at 800 K, if the thermal conductivity ( $\kappa$ ) is assumed to be unaffected by grain texturing and also the resistivity ratio ( $\rho_{\text{CS}}/\rho_{\text{HP}}$ ) is assumed to be independent of temperature.